DOI: 10.61782/fa.2023.0776

forum acusticum 2023

VALIDATION OF THE SOURCE LOCALIZATION METHOD SODIX FOR COHERENT SOUND SOURCES

Sebastian Oertwig[1*] **and Henri Siller**[1]
[1] German Aerospace Center (DLR), Berlin, Germany

ABSTRACT

A new validation of the source localization method SODIX for coherent sound sources is presented. The DLR fan noise prediction tool PropNoise is used to model the tonal noise of a low-speed fan stage that is generated by the interaction of the rotor wakes with the stator vanes. The simulated data is used to evaluate the capabilities of the source localization method SODIX to determine the coherent sound radiation from the intake and the nozzle exit. The analysis technique includes a parameterization of the source directivities using cubic B-splines. A parametric study on the number of base elements is carried out for the simulated tones with different radiation patterns. The results show that SODIX is able to accurately reproduce the coherent sound radiation of the simulated tones from the intake and the nozzle exit. The results also indicate that a number of base elements from 20 to 100 is a reasonable choice for a large frequency range.

Keywords: *source localization, source coherence, tonal noise, engine acoustics, compressed sensing*

1. INTRODUCTION

The source localization method SODIX is able to determine the positions and the directivities of sound sources based on microphone array measurements. SODIX stands for *SOurce DIrectivity modelling in the cross-spectral matriX* and is mainly being developed for the analysis of broadband noise sources in static engine noise testing, see [1–3]. The method is able to quantify the contribution of individual source regions to the overall radiated noise.

SODIX has originally been developed for the analysis of broadband noise sources and initially used an incoherent source model. An extension of the method for fully and partially coherent sound sources has recently been presented [4]. The application of the method to a fan tone measured during an outdoor engine noise test has shown that a coherent source model improves the source localization for engine tones that radiate coherently from the intake and the nozzle exit [5]. The results proved the possibility to apply SODIX to engine tones and other potentially coherent sound sources.

The SODIX method for coherent sound sources is based on a coherent source model, a compressed sensing based algorithm, and a parameterization of the source directivities with base functions. The influence of the number of base elements on the localization results has not yet been studied. Therefore, this paper presents a new validation of SODIX for coherent sound sources with simulated data. The tonal noise of a low-speed fan stage generated by the interaction of the rotor wakes with the stator vanes is modeled with the DLR fan noise prediction tool PropNoise. The sources are propagated from the ducted fan stage to microphone positions that are used for the source localization. The capability of the source localization method SODIX to determine the coherent sound radiation from the intake and the nozzle exit will be investigated by comparing the derived source directivities with the simulated data. Different error measures are used to quantify the performance of the source localization.

This paper is organized as follows: section 2 provides a description of the source localization method SODIX for coherent sound sources, section 3 presents the PropNoise simulation, section 4 shows the source localization results derived with SODIX, and section 5 concludes this paper and provides an outlook for future research.

*Corresponding author: sebastian.oertwig@dlr.de.

2. METHODOLOGY

This section provides a description of the source localization method SODIX for coherent sound sources. The analysis technique is based on a directive source model for coherent sound sources, the parameterization of the source directivities with base functions, and the use of a compressed sensing based algorithm.

2.1 The source localization method SODIX

In comparison to other source localization methods, SODIX uses a special point source model to describe the amplitudes and the directivities of the sound sources. The method fits a model of the complex sound pressure vector or the cross-spectral matrix to measured microphone data. Different source models can be used for incoherent, partially coherent, and fully coherent sound sources [5]. In all cases, SODIX models a set of equivalent point sources with individual amplitudes from all sources towards all microphones, as shown in Fig. 1 for a single point source with two distinct radiation lobes.

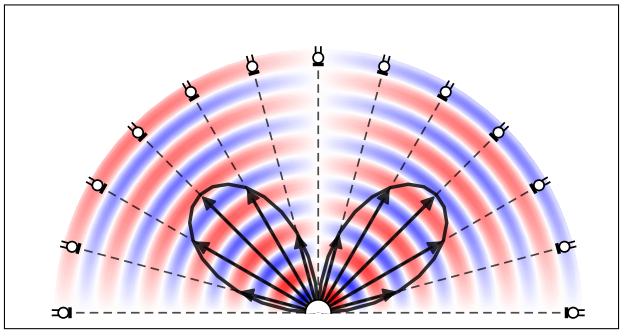

Figure 1: Directive point sources used in the source localization method SODIX with individual amplitude for every microphone.

2.2 SODIX source model for coherent sound sources

The use of a source model that allows for source coherence is a prerequisite for the analysis of engine tones because the sound radiation of the tones from the engine intake and the nozzle exit can be at least partially coherent. A thorough description of the extension of SODIX for coherent sound sources has been presented recently [5]. This paper provides an overview of the methodology for the sake of completeness.

In the case of fully coherent sound sources, it is sufficient to model the complex sound pressure vector $\mathbf{p}^{\text{mod}}$ at the microphones by

$$\mathbf{p}^{\text{mod}} = \hat{\mathbf{G}}\hat{\mathbf{D}} \,, \tag{1}$$

with $\hat{\mathbf{G}} \in \mathbb{C}^{M\times MJ}$ being the transfer matrix that contains the free-field Green's functions and $\hat{\mathbf{D}} \in \mathbb{C}^{MJ}$ being the unknown source directivities for all sources $j = 1, \ldots, J$ pointing to all microphones $m = 1, \ldots, M$. The transfer matrix $\hat{\mathbf{G}}$ and the solution vector $\hat{\mathbf{D}}$ have a block structure that can be exploited for efficient solving.

The modeled pressure vector $\mathbf{p}^{\text{mod}}$ in Eqn. (1) can be compared with the measured spectra $\mathbf{p} = [p_1, \ldots, p_M]^T$ at the microphones in order to determine the unknown source directivities. However, the dimension of the transfer matrix shows that the equation system is underdetermined because in practical applications the number of microphones is much lower than the number of source directivities to be determined: $M \ll MJ$. Therefore, a parameterization of the source directivities with base functions is introduced that leads to a significant reduction of the degree of freedom in the modeling of the sound sources compared to a free modeling of the directivities without parameterization.

2.3 Parameterization of the source directivities

The directivity of a single source is now expressed as a weighted sum of L elements of the base function $\mathbf{B}$:

$$D_{jm} = \sum_{l=1}^{L} x_{jl} B_l \left(\tilde{\theta}_{jm}\right) \,, \tag{2}$$

where x_{jl} is a weighting factor of the base element B_l and becomes the new variable to be solved for. The base elements are evaluated at specific coordinates $\tilde{\theta}$ for each combination of point source j and microphone m. A parameterization over the local emission angle θ is used that is defined as the angle between the engine centerline and the connecting line from a source to a microphone. Without loss of generality, the angle is further normalized to the unit interval $\tilde{\theta} \in [0, 1]$ by its minimum and maximum value.

The parameterized localization problem is given after inserting Eqn. (2) into the original problem formulation from Eqn. (1):

$$\begin{aligned} \mathbf{p}^{\text{mod}} &= \hat{\mathbf{G}}\hat{\mathbf{D}} \\ &= \hat{\mathbf{G}}\hat{\mathbf{B}}\hat{\mathbf{x}} \\ &= \boldsymbol{\Psi}\hat{\mathbf{x}} \,, \end{aligned} \tag{3}$$

where $\hat{\mathbf{x}} \in \mathbb{C}^{LJ}$ is the new solution vector with the weighting factors of the base elements, $\hat{\mathbf{B}} \in \mathbb{C}^{MJ \times LJ}$ is a block-diagonal matrix that contains the base functions and connects the weights $\hat{\mathbf{x}}$ with the source directivities $\hat{\mathbf{D}}$, and $\mathbf{\Psi} = \hat{\mathbf{G}}\hat{\mathbf{B}} \in \mathbb{C}^{M \times LJ}$ is the new transfer matrix that consists of the known sound propagation $\hat{\mathbf{G}}$ and the base functions $\hat{\mathbf{B}}$.

A comparison of the dimensions of the transfer matrix without parameterization $\hat{\mathbf{G}}$ and the transfer matrix with parameterization $\mathbf{\Psi}$ shows that a significant reduction of the degree of freedom in the modeling of the source directivities can be achieved when the number of base elements is much lower than the number of array microphones: $L \ll M$. This paper provides further guidelines on how to select the number of base elements L.

A new parameterization of the source directivities with cubic B-splines is presented. Figure 2 shows the elements B_l^3 of the cubic B-splines on the unit interval for a number of $L = 11$ elements. The individual base elements have local support, i.e. they only affect a short interval of the domain.

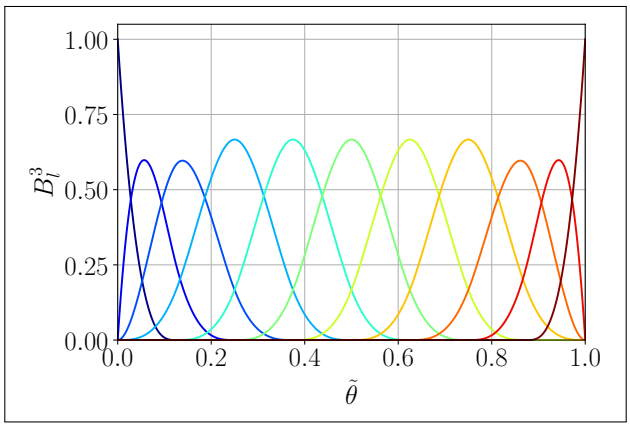

Figure 2: Base elements of the cubic B-splines.

Figure 3 shows the parameterization of a simulated source directivity that has been modeled using the DLR fan noise prediction tool PropNoise, see section 3. In this example, the parameterization with cubic B-splines (dark, thin line) is able to reproduce the amplitude (top) and the phase (bottom) of the simulated source directivity (light, thick line) over a large angular and dynamic range. In this case, the simulated source directivity has distinct phase jumps between the radiation lobes at normalized angles of $\tilde{\theta} \approx 0.6$ and $\tilde{\theta} \approx 0.8$ that are attributed to the directivity of different radial modes. The correct determination of the phase is crucial for coherent sound sources because the phase does affect the sound pressure levels in the far-field, in contrast to incoherent sound sources.

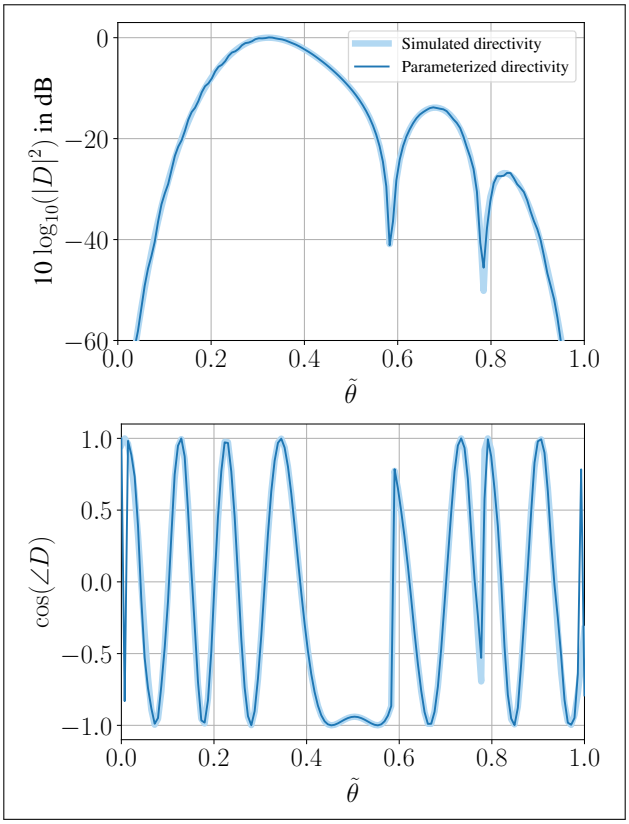

Figure 3: Parameterization of a simulated source directivity with cubic B-splines regarding its amplitude (top) and phase (bottom).

2.4 Compressed sensing based algorithm

The parameterized equation system (3) is still underdetermined because in practical applications, the number of microphones is lower than the number of unknown parameterized source amplitudes: $M \ll JL$. Therefore, a compressed sensing based algorithm is used to determine the unknown source directivities. Compressed sensing allows to reconstruct sparse signals [6]. The sparsity of the source distribution is a good assumption for the sound radiation of tones from turbofan engines as fan tones radiate from distinct locations like the intake and the nozzle exit.

One algorithm that is very suitable for the analysis of engine tones with SODIX is the *Block Orthogonal Matching Pursuit* (BOMP) [7], which exploits the block struc-

ture of the transfer matrix and the solution vector. The corresponding minimization problem is given by

$$\hat{\mathbf{x}} = \underset{\mathbf{x_j} \in \mathbb{C}^M}{\arg\min} \ \|\mathbf{x_j}\|_1 \ \text{s.t.} \ \|\mathbf{p} - \mathbf{\Psi}\hat{\mathbf{x}}\|_2 \leq \epsilon \,, \qquad (4)$$

where $\mathbf{x_j}$ are the weighting factors of the directivity of the point source j. Eqn. (4) promotes sparsity on the number of sources used for the reconstruction of the sound field, but not on their directivity which is fully recovered. The parameter ϵ is an error bound, e.g. the energy of additional measurement noise.

Algorithm 1 shows the iterative procedure of the BOMP, where $\mathbf{r}$ is the residuum between measured and modeled sound pressure vectors, $\mathbf{\Psi_j} \in \mathbb{C}^{M \times L}$ is a submatrix of the transfer matrix corresponding to the source j, $\mathbf{\Psi}^{\dagger R} = \mathbf{\Psi}^H \left(\mathbf{\Psi}\mathbf{\Psi}^H + \sigma \mathbf{I}\right)^{-1}$ is a regularized pseudo-inverse of the transfer matrix, S is the set of determined indices i of the dominant blocks, s is the maximum number of blocks that can be recovered, t is an iteration index, ϵ is a stopping criterion, and $\|\cdot\|_2$ is the Euclidean norm.

Algorithm 1 Block Orthogonal Matching Pursuit

Require: $\mathbf{p}$, $\mathbf{\Psi}$

Ensure: $\mathbf{r}^{(0)} = \mathbf{p}$, $\hat{\mathbf{x}}^{(0)} = \mathbf{0}$, $S^{(0)} = \emptyset$

1: $t \leftarrow 1$
2: **while** $\left\|\mathbf{r}^{(t)}\right\|_2 > \epsilon$ and $t \leq s$ **do**
3: $\quad i^{(t)} \leftarrow \arg\max_j \left(\left\|\mathbf{\Psi_j}^H \mathbf{r}^{(t-1)}\right\|_2\right)$
4: $\quad S^{(t)} \leftarrow S^{(t-1)} \cup i^{(t)}$
5: $\quad \hat{\mathbf{x}}_S^{(t)} \leftarrow \mathbf{\Psi}_S^{\dagger R}\mathbf{p}$
6: $\quad \mathbf{r}^{(t)} \leftarrow \mathbf{p} - \mathbf{\Psi}\hat{\mathbf{x}}_S^{(t)}$
7: $\hat{\mathbf{x}}_W \leftarrow \mathbf{\Psi}^{\dagger R}\mathbf{r}$
8: $\hat{\mathbf{x}} \leftarrow \hat{\mathbf{x}}_S + \hat{\mathbf{x}}_W$
9: **return** $\hat{\mathbf{x}}$

The BOMP algorithm finds the dominant blocks of the transfer matrix one after the other by correlation with the current residuum. The weighting factors $\hat{\mathbf{x}}$ of the base functions are determined by inverting the linear equation system using the regularized pseudo-inverse of the transfer matrix $\mathbf{\Psi}_S^{\dagger R}$ for the dominant blocks. The regularized pseudo-inverse of the transfer matrix includes an additional L_2 regularization that helps to find stable solutions even for high condition numbers of the transfer matrix. The regularization parameter σ is determined from the measurements and the transfer matrix using a Bayesian approach [8]. An additional analysis step is performed at the end of the BOMP algorithm that estimates remaining, weak sources based on the residuum and the full transfer matrix. Finally, the solution $\hat{\mathbf{x}}_S$ for the dominant sources and the solution $\hat{\mathbf{x}}_W$ for the weak sources are added up.

BOMP and related compressed sensing based algorithms have successfully been applied at DLR for the detection of induct modes in turbo-machines [9–12].

3. SIMULATION OF FAN TONES

A simulation of the tonal noise of a low-speed fan stage is used to validate the source localization method SODIX for coherent sound sources. The fan tones generated by the interaction of the rotor wakes with the stator vanes are analytically modeled using the DLR fan noise prediction tool *PropNoise* [13]. The following section describes the simulation setup and the properties of the simulated tones.

3.1 Setup of the simulation

Figure 4 shows a schematic of the PropNoise simulation of the interaction tones for a low-speed fan stage inside an annular duct [14]. The tones are propagated from the fan stage inside the duct to the engine inlet further upstream at $x = -6\,\mathrm{m}$ and to the nozzle exit further downstream at $x = 0\,\mathrm{m}$. No additional damping of the sound field e.g. by considering acoustic liners inside the duct has been modeled. Outside the duct, the sound field is propagated to microphone positions that are used for the source localization with SODIX. The radiation of the tones into the far-field is described by an analytical model with the solution to the Kirchhoff-Helmholtz integral [15].

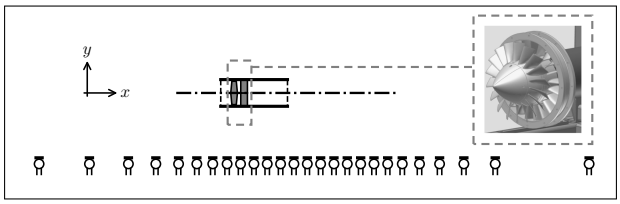

Figure 4: Setup of the PropNoise simulation of the interaction tones for a low-speed fan stage [14]. The schematic only shows every tenth microphone. Dimensions are not to scale.

A linear microphone array in parallel with the engine axis is used for the source localization with SODIX. The array consists of 252 microphones that provide a polar resolution of approximately $0.6°$. The array covers the polar

range from 25° to 155°. The lateral distance of the microphone array to the engine axis is approximately 6.6 m. This microphone setup is similar to that at a static engine noise test on a free-field teststand [3].

3.2 Properties of the simulated tones

The interaction of the rotor wakes with the stator vanes generates tones at the blade passing frequencies (BPF). These frequencies only depend on the number of rotor blades and the rotational speed of the fan. The interaction tones are dominated by Tyler-Sofrin modes [16] with azimuthal mode orders m that can be analytically described by the number of rotor blades B and the number of stator vanes V:

$$m = hB \pm kV \ , \tag{5}$$

where h is a positive integer that corresponds to the order of the BPF harmonic and $k \in \mathbb{Z}$ is an integer.

PropNoise calculates the sound pressure $p_m\left(f, \tilde{\theta}\right)$ as a function of the mode order m, the frequency f and the emission angle $\tilde{\theta}$. The complex sound pressures of the individual modes are then coherently superimposed at the microphone positions in order to derive input data for the source localization with SODIX:

$$p\left(f, \tilde{\theta}\right) = \sum_m p_m\left(f, \tilde{\theta}\right) \ . \tag{6}$$

In this simulation, the interaction tones have been calculated up to the tenth BPF, with the first BPF at a frequency of 512 Hz. The number of cut-on azimuthal mode orders varies from one at low frequencies to four at the highest frequencies. The radiation pattern of the tones in the far-field also depend on the number of radial modes that are cut-on.

4. RESULTS

This section presents the source localization results derived with SODIX. First, section 4.1 shows example localization results for two different frequencies with a selected number of base elements. Then, a parametric study on the number of base elements over a wide frequency range is presented in section 4.2.

4.1 Example source localization results

Figure 5 and 6 show example source localization results derived with SODIX for 2BPF and 8BPF of the simulated interaction tones, respectively.

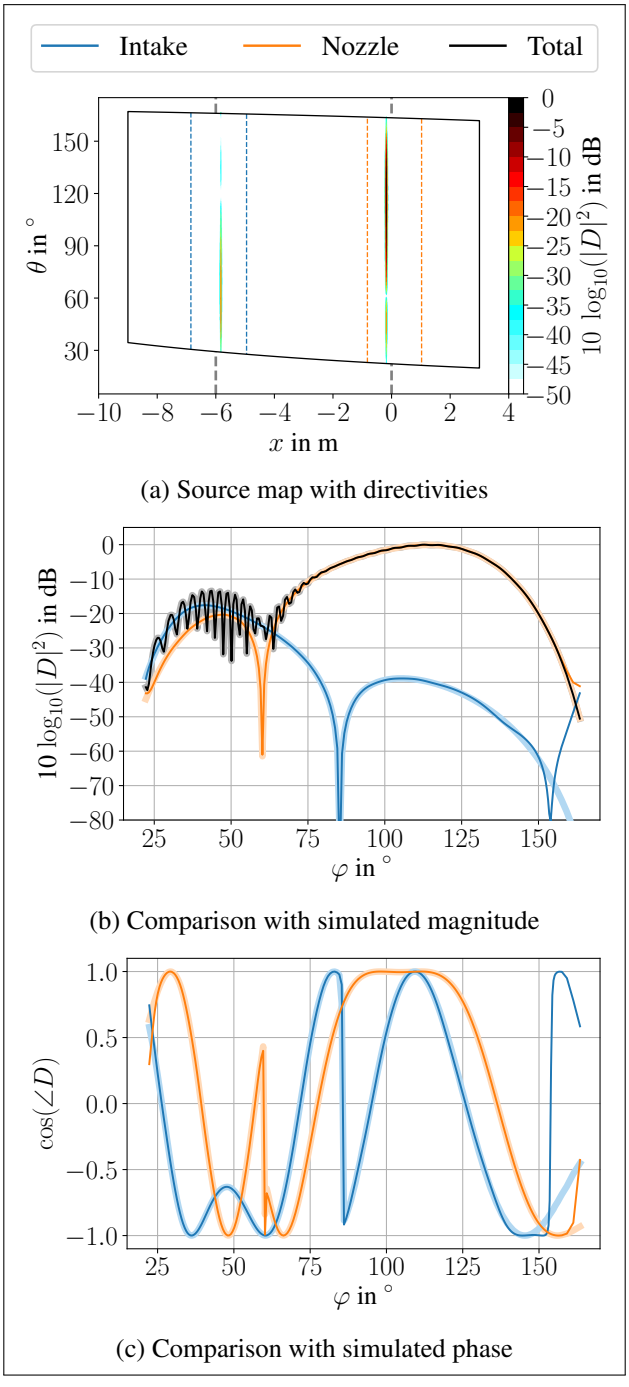

(a) Source map with directivities

(b) Comparison with simulated magnitude

(c) Comparison with simulated phase

Figure 5: Source localization results derived with SODIX for 2BPF of the simulated interaction tones. The dashed lines in the source map show the integration areas around the intake (blue) and the nozzle (orange).

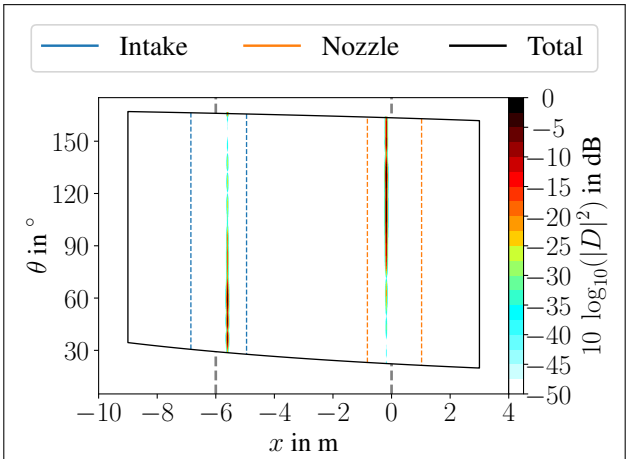

(a) Source map with directivities

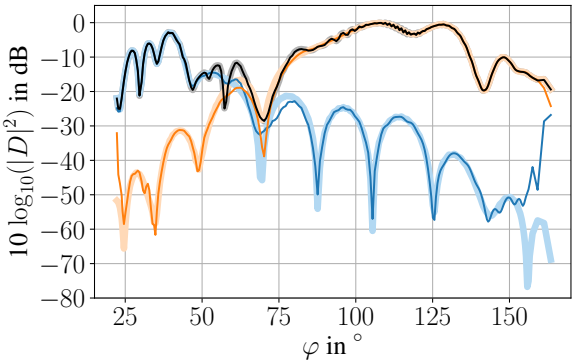

(b) Comparison with simulated magnitude

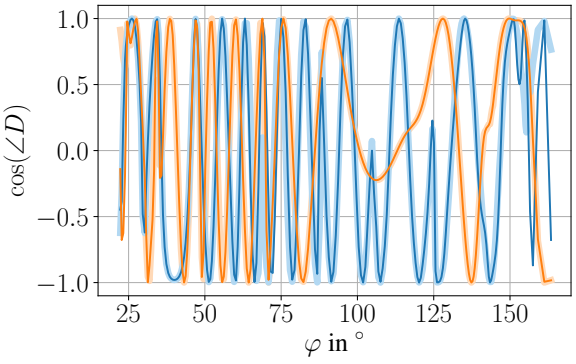

(c) Comparison with simulated phase

Figure 6: Source localization results derived with SODIX for 8BPF of the simulated interaction tones. The dashed lines in the source map show the integration areas around the intake (blue) and the nozzle (orange).

Figure 5 and 6 present typical source maps (top) with the directive source amplitudes over the source position on the horizontal axis and the emission angle on the vertical axis. The grey, dashed lines at $x = -6\,\mathrm{m}$ and $x = 0\,\mathrm{m}$ indicate the positions of the intake and the nozzle exit, and the colored, dashed lines indicate the integration areas around the intake and the nozzle exit used to extract the derived source amplitudes for comparison with the simulated levels. Both figures show this quantitative comparison of the magnitude (center) and the phase (bottom) of the derived source directivities (dark, thin lines) with the simulated sources (light, thick lines). The results were derived with $L = 30$ base elements for 2BPF and $L = 85$ base elements for 8BPF.

The localization results clearly show that SODIX is able to accurately determine the coherent sound radiation from the intake and the nozzle exit. In both cases, SODIX determines a point source at the correct position near the intake and the nozzle. The derived source directivities also agree well with the simulated sources in terms of their magnitude and phase over a large angular range. SODIX even reproduces the phase jumps between the radiation lobes. Some deviations of the derived directivities from the simulated levels occur at both ends of the microphone array where the spatial resolution is lower. The source localization results can depend on the selected number of base elements, as shown in the following.

4.2 Parametric study on the number of base elements

A parametric study on the number of base elements used for the parameterization of the source directivities in SODIX has been carried out for a wide frequency range up to 10BPF. The number of base elements L has been systematically varied from 5 to 100. The quality of the source localization with SODIX is evaluated by comparing the derived directivities with the simulated levels using the error measure

$$\varepsilon_1 = \frac{1}{M} \sum_{\varphi=\varphi_1}^{\varphi_M} \left| 10 \log_{10} \left(\frac{p^2(\varphi)}{p^2_{\mathrm{sim}}(\varphi)} \right) \right| . \qquad (7)$$

The error ε_1 measures the average deviation between derived and simulated source directivities over their full dynamic range. The error measure is applied to the total sound pressure level and to the individual contribution from the intake and the nozzle, respectively. Figure 7 shows the results of the parametric study.

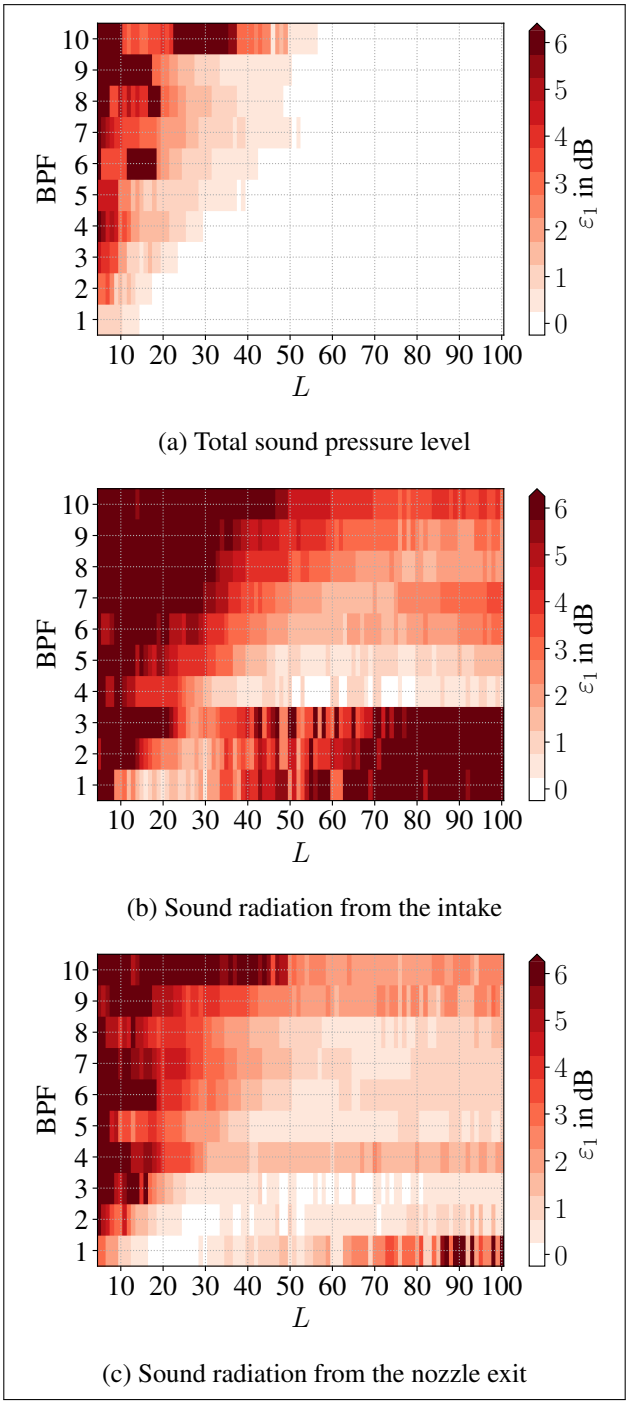

(a) Total sound pressure level

(b) Sound radiation from the intake

(c) Sound radiation from the nozzle exit

Figure 7: Error ε_1 for the total sound pressure level (top) and the individual sound radiation from the intake (center) and the nozzle exit (bottom).

Figure 7 shows the average reproduction error ε_1 over the number of base elements L on the horizontal axis and the different tones on the vertical axis for the total sound pressure level (top) and for the sound radiation from the intake (center) and the nozzle exit (bottom).

The results in Fig. 7a show that the total sound pressure levels at the microphones are well reproduced when the number of base elements is large enough. The results for the individual sound radiation from the intake and the nozzle in Fig. 7b and Fig. 7c indicate that a minimum number of base elements from 20 to 80 is required to accurately reproduce the coherent sound radiation of the tones. The results demonstrate that the minimum number of base elements increases with the frequency and the complex radiation pattern of the tones. The radiation lobes of the tones are not well reproduced with fewer base elements. At the same time, a very high number of base elements can be disadvantageous for the source localization with SODIX. For low frequencies and high numbers of base elements, the derived source directivities tend to oscillate around the simulated levels which leads to larger deviations. This phenomenon is well known from polynomial interpolation as Runge's phenomenon [17].

The average reproduction error ε_1 for the sound radiation from the nozzle is mainly below 1 dB and that for the sound radiation from the intake mainly below 2 dB, if the minimum number of base elements is exceeded and no over-fitting occurs. The sound radiation from the nozzle is in general better reproduced than that from the intake because it is the dominant source in these simulations. The average reproduction error also increases with the frequency due to the constant spatial resolution of the microphone array.

The source localization results from the previous section have shown that the deviations from the simulated levels mainly occur at low source levels at both ends of the microphone array. The main lobes of the tones are even better reproduced with SODIX than the average reproduction error suggests.

5. CONCLUSIONS AND OUTLOOK

A new validation of the source localization method SODIX for coherent sound sources with simulated fan tones has been presented. The results show that SODIX accurately reproduces the coherent sound radiation of the simulated tones from the intake and the nozzle exit. The results also indicate that a number of base elements from 20 to 100 is a good choice for a large frequency range.

Future modifications of this simulation are possible, e.g. by including acoustic liners in the duct, simulating a partially coherent sound radiation from the intake and the nozzle exit, or considering other microphone positions.

In general, the results of the validation confirm the possibility to apply SODIX to engine tones and other potentially coherent sound sources.

6. ACKNOWLEDGMENTS

The research leading to these results has received funding from the German Federal Ministry for Economic Affairs and Climate Action (BMWK) in the framework of the LuFo project MUTE under the grant agreement number 20T1915D. The authors would like to thank Maximilian Behn, Sébastien Guérin, Antoine Moreau, and Stephen Schade from DLR Berlin for the various discussions and the provision of the simulated data from PropNoise.

7. REFERENCES

[1] U. Michel and S. Funke, "Noise Source Analysis of an Aeroengine with a New Inverse Method SODIX," in *14th AIAA/CEAS Aeroacoustics Conference (29th AIAA Aeroacoustics Conference), May 5-7, 2008, Vancouver, British Columbia*, no. AIAA 2008-2860.

[2] S. Funke, A. Skorpel, and U. Michel, "An extended formulation of the SODIX method with application to aeroengine broadband noise," in *18th AIAA/CEAS Aeroacoustics Conference, 4-6 June 2012, Colorado Springs, USA*, no. AIAA 2012-2276.

[3] S. Funke, *Ein Mikrofonarray-Verfahren zur Untersuchung der Schallabstrahlung von Turbofantriebwerken*. Doctoral thesis, Technische Universität Berlin, 2017.

[4] S. Oertwig, H. Siller, and S. Funke, "SODIX for fully and partially coherent sound sources," in *9th Berlin Beamforming Conference, 8-9 June, 2022, Berlin*.

[5] S. Oertwig, H. A. Siller, T. Schumacher, and S. Funke, "Extension of the source localization method SODIX for the determination of partially coherent sound sources," in *28th AIAA/CEAS Aeroacoustics Conference, June 14-17, 2022, Southampton, UK*.

[6] D. L. Donoho, "Compressed sensing," *IEEE Transactions on Information Theory*, vol. 52, no. 4, pp. 1289–1306, 2006.

[7] Y. C. Eldar, P. Kuppinger, and H. Bolcskei, "Block-sparse signals: Uncertainty relations and efficient recovery," *IEEE Transactions on Signal Processing*, vol. 58, no. 6, pp. 3042–3054, 2010.

[8] J. Hurst, M. Behn, L. Klähn, and U. Tapken, "Accuracy and robustness of sparse reconstruction techniques for azimuthal mode analysis of in-duct sound fields," *Journal of Sound and Vibration*, vol. 534, p. 117011, 2022.

[9] R. Kisler, "Azimutale Modalanalyse akustischer Signale in zylindrischen Kanälen bei Unterabtastung mittels Compressed Sensing," Master thesis, Technische Universität Berlin, 2016.

[10] M. Behn, R. Kisler, and U. Tapken, "Efficient azimuthal mode analysis using compressed sensing," in *22nd AIAA/CEAS Aeroacoustics Conference, 30 May - 1 Jun 2016, Lyon, France*.

[11] M. Behn, B. Pardowitz, and U. Tapken, "Compressed sensing based radial mode analysis of the broadband sound field in a low-speed fan test rig," in *7th Berlin Beamforming Conference, March 5-6, 2018*.

[12] J. Hurst, M. Behn, U. Tapken, and L. Enghardt, "Sound power measurements at radial compressors using compressed sensing based signal processing methods," in *ASME Turbo Expo 2019: Turbomachinery Technical Conference and Exposition, 17–21 June, 2019, Phoenix, USA*.

[13] A. Moreau, *A unified analytical approach for the acoustic conceptual design of fans of modern aeroengines*. PhD thesis, Technische Universität Berlin, 2017.

[14] S. Schade, R. Jaron, A. Moreau, and S. Guérin, "Mechanisms to reduce the blade passing frequency tone for subsonic low-count OGV fans," *Aerospace Science and Technology*, vol. 125, p. 107083, 2022.

[15] S. Lewy, "Prediction of turbofan rotor or stator broadband noise radiation," *Acta Acustica united with Acustica*, vol. 93, pp. 275–283.

[16] J. Tyler and T. Sofrin, "Axial flow compressor noise studies," tech. rep., SAE Technical Paper 620532, 1962.

[17] C. Runge, "Über empirische Funktionen und die Interpolation zwischen äquidistanten Ordinaten," in *Zeitschrift für Mathematik und Physik*, vol. 46, B. G. Teubner, 1901.